Vet. Res. (2010) 41:03
DOI: 10.1051/vetres/2009051

www.vetres.org

Original article

Effects of growth conditions on biofilm formation by *Actinobacillus pleuropneumoniae*

Josée Labrie[1], Geneviève Pelletier-Jacques[1], Vincent Deslandes[1], Mahendrasingh Ramjeet[1], Eliane Auger[1], John H.E. Nash[2], Mario Jacques[1*]

[1] Groupe de recherche sur les maladies infectieuses du porc et Centre de recherche en infectiologie porcine, Faculté de médecine vétérinaire, Université de Montréal, 3200 Sicotte, St-Hyacinthe, Québec, Canada J2S 7C6
[2] Office of Biotechnology, Genomics and Population Health, Public Health Agency of Canada, Ottawa, Ontario, Canada K1A 0K9

(Received 24 April 2009; accepted 8 September 2009)

Abstract – Biofilm formation is an important virulence trait of many bacterial pathogens. It has been reported in the literature that only two of the reference strains of the swine pathogen *Actinobacillus pleuropneumoniae*, representing serotypes 5b and 11, were able to form biofilm in vitro. In this study, we compared biofilm formation by the serotype 1 reference strain S4074 of *A. pleuropneumoniae* grown in five different culture media. We observed that strain S4074 of *A. pleuropneumoniae* is able to form biofilms after growth in one of the culture conditions tested brain heart infusion (BHI medium, supplier B). Confocal laser scanning microscopy using a fluorescent probe specific to the poly-N-acetylglucosamine (PGA) polysaccharide further confirmed biofilm formation. In accordance, biofilm formation was susceptible to dispersin B, a PGA hydrolase. Transcriptional profiles of *A. pleuropneumoniae* S4074 following growth in BHI-B, which allowed a robust biofilm formation, and in BHI-A, in which only a slight biofilm formation was observed, were compared. Genes such as *tadC*, *tadD*, genes with homology to autotransporter adhesins as well as genes *pgaABC* involved in PGA biosynthesis and genes involved in zinc transport were up-regulated after growth in BHI-B. Interestingly, biofilm formation was inhibited by zinc, which was found to be more present in BHI-A (no or slight biofilm) than in BHI-B. We also observed biofilm formation in reference strains representing serotypes 3, 4, 5a, 12 and 14 as well as in 20 of the 37 fresh field isolates tested. Our data indicate that *A. pleuropneumoniae* has the ability to form biofilms under appropriate growth conditions and transition from a biofilm-positive to a biofilm-negative phenotype was reversible.

Actinobacillus pleuropneumoniae **/ biofilm / growth condition / transcriptomic**

1. INTRODUCTION

Actinobacillus pleuropneumoniae, a member of the *Pasteurellaceae*, is an important swine pathogen responsible for economic losses in the swine industry. To date, 15 serotypes of *A. pleuropneumoniae* have been described based on capsular antigens [3, 10]. The virulence of the bacteria is mediated by the coordinated action of several virulence factors, namely the capsule, lipopolysaccharides (LPS), Apx toxins and outer membrane proteins involved in iron uptake [4, 11, 14, 18, 19, 28, 29].

It is widely accepted that the majority of bacteria in virtually all ecosystems (natural,

* Corresponding author: mario.jacques@umontreal.ca

engineered and pathogenic ecosystems) grow in matrix-enclosed biofilms [7]. The matrix provides biofilm cells with a protected microenvironment containing nutrients, secreted enzymes and DNA. The matrix also contributes to the increased resistance to antibiotics and host defenses exhibited by biofilm cells [15]. All members of the *Pasteurellaceae* are inhabitants of mucosal surfaces of mammals and therefore formation of a biofilm may be crucial to their persistence in vivo. However, biofilms have only been investigated in a few species of the *Pasteurellaceae* family [16]. In *A. pleuropneumoniae*, the formation of biofilms on polystyrene microtiter plate is dependent on the production of poly-N-acetylglucosamine (PGA) a linear polymer of N-acetylglucosamine residues in β(1,6) linkage [17, 20]. The production of PGA is encoded by the genes *pgaABCD* [20]. A novel insertion element, ISApl1, was recently identified in an A/T rich region of the *pgaC* gene of the biofilm-negative *A. pleuropneumoniae* strain HB04 [25]. PGA is a substrate for dispersin B (DspB), a biofilm-releasing glycosyl hydrolase produced by *Aggregatibacter* (*Actinobacillus*) *actinomycetemcomitans* and *A. pleuropneumoniae* [20, 22]. It has also been reported that only 2 of the 15 *A. pleuropneumoniae* reference strains, representing serotypes 5b and 11, were able to form a biofilm in vitro and that the transition from a biofilm-positive to biofilm-negative phenotype was irreversible [21]. However, Li et al. [24] recently observed slight biomass of biofilm when the *A. pleuropneumoniae* serotype 1 reference strain S4074 was grown in serum-free TSB but not in serum-containing TSB. In addition, an enhanced biofilm formation was observed in *luxS* [24] and *hns* [8] mutants of *A. pleuropneumoniae* strain S4074.

The aims of the present study were: (i) to re-evaluate biofilm formation by *A. pleuropneumoniae* reference strain S4074 (serotype 1) under different growth conditions using a standard microtiter plate and crystal violet staining protocol; (ii) to evaluate the ability of 16 reference strains and 37 fresh field isolates to form biofilm in the growth condition shown to allow the best biofilm formation and (iii) to determine the transcriptomic profile of *A. pleuropneumoniae* strain S4074 when grown in that culture condition.

2. MATERIALS AND METHODS

2.1. Bacterial strains and growth conditions

Bacterial strains used in the present study are listed in Table I. Bacteria were grown on brain heart infusion agar plates (BHI; Difco Laboratories, Detroit, MI, USA) supplemented with 15 μg/mL nicotinamide adenine dinucleotide (NAD). A colony was transferred into 5 mL of Luria-Bertani broth (LB; Difco), tryptic soy broth (TSB; Difco), Mueller Hinton broth (MH; Difco) or BHI (BHI-A; Difco or BHI-B; Oxoid Ltd, Basingstoke, Hampshire, UK) with 5 μg/mL NAD and incubated at 37 °C overnight with agitation. This culture was used for the biofilm assays.

2.2. Biofilm assay in microtiter plates

The microtiter plate biofilm assay is a static assay particularly useful for examining early events in biofilm formation [27]. The wells of a sterile 96-well microtiter plate (Costar® 3599, Corning, NY, USA) were filled in triplicate with a dilution (1/100) of an overnight bacterial culture. Following an incubation of 6 or 24 h at 37 °C, the wells were washed by immersion in water and excess water was removed by inverting plates onto a paper towel. The wells were then filled with 100 μL of crystal violet (0.1%) and the plate was incubated for 2 min at room temperature. After removal of the crystal violet solution, the plate was washed and dried in a 37 °C incubator for 30 min and 100 μL of ethanol (70%) were added to the wells. Absorbance was measured at 590 nm using a spectrophotometer (Powerwave, BioTek Instruments, Winooski, VT, USA).

2.3. Scanning laser confocal microscopy

The same biofilm assay protocol was used as described previously. After the 6 or 24 h incubation, the wells were filled with 100 μL of Wheat Germ Agglutinin (WGA)–Oregon Green 488 (Molecular Probes, Eugene, OR, USA) diluted 1/100 in PBS and the plate was incubated for 30 min at room temperature in the dark. The plate was then washed with water and filled with PBS. The plate was observed with a confocal microscope (Olympus FV1000

Table I. *A. pleuropneumoniae* strains used in the present study.

Strains	Relevant traits	Source
Reference strains		
S4074	Serotype 1	K.R. Mittal[1]
4226	Serotype 2	K.R. Mittal[1]
1421	Serotype 3	K.R. Mittal[1]
1462	Serotype 4	K.R. Mittal[1]
K17	Serotype 5a	K.R. Mittal[1]
L20	Serotype 5b	K.R. Mittal[1]
FEMO	Serotype 6	K.R. Mittal[1]
WF.83	Serotype 7	K.R. Mittal[1]
405	Serotype 8	K.R. Mittal[1]
13261	Serotype 9	K.R. Mittal[1]
13039	Serotype 10	K.R. Mittal[1]
56153	Serotype 11	K.R. Mittal[1]
832985	Serotype 12	K.R. Mittal[1]
N273[4]	Serotype 13	M. Gottschalk[1]
3906[4]	Serotype 14	M. Gottschalk[1]
HS143	Serotype 15	M. Gottschalk[1]
Field strains		
05-7430, 05-7431	Serotype 1	M. Ngeleka[2]
111A, 719, 2398, 2521	Serotype 1	D. Slavic[3]
05-4817, 05-C996, 06-996	Serotype 5a	S. Messier[1]
04-37943, 04-3128, 05-508	Serotype 5a	M. Ngeleka[2]
05-6501, 06-4091	Serotype 5b	S. Messier[1]
03-14796, 03-22382, 03-22383, 05-4832	Serotype 5b	M. Ngeleka[2]
366A, 400, 564D, 888	Serotype 5b	D. Slavic[3]
05-3695, 06-3008, 06-3060, 06-4108	Serotype 7	S. Messier[1]
04-37257, 05-14401	Serotype 7	M. Ngeleka[2]
881, 986, 1951, 4648	Serotype 7	D. Slavic[3]
05-13146, 05-14657, 05-20080, 05-20081, 05-2983	Serotype 15	M. Ngeleka[2]

[1] Faculté de médecine vétérinaire, Université de Montréal, St-Hyacinthe, QC, Canada.
[2] Prairie Diagnostic Services, University of Saskatchewan, Saskatoon, SK, Canada.
[3] Ontario Veterinary College, University of Guelph, Guelph, ON, Canada.
[4] These strains are NAD-independent and belong to biotype II.

IX81). WGA was excited at 488 nm and detected using 520 nm filters. The images were processed using Fluoview software (Olympus).

2.4. Transcriptomic microarray experiments

2.4.1. RNA extractions

For the microarray experiments, BHI-A or BHI-B broths were inoculated with 500 µL of an overnight culture of *A. pleuropneumoniae* serotype 1 strain S4074 and grown at 37 °C in an orbital shaker until an optical density of 0.6 was reached. Ice-cold RNA degradation stop solution (95% ethanol, 5% buffer-saturated phenol), shown to effectively prevent RNA degradation and therefore preserve the integrity of the transcriptome [2], was added to the bacterial culture at a ratio of 1:10 (vol/vol). The sample was mixed by inversion, incubated on ice for 5 min, and then spun at 5 000 *g* for 10 min to pellet the cells. Bacterial RNA isolation was then carried out using the QIAGEN RNeasy MiniKit (QIAGEN, Mississauga, ON, Canada), as prescribed by the manufacturer. During the extraction, samples were subjected to

an on-column DNase treatment, as suggested by the manufacturer and then treated with Turbo DNase (Ambion, Austin, TX, USA) to ensure that all DNA contaminants were eliminated. The RNA concentration, quality and integrity were assessed spectrophotometrically and on gel.

2.4.2. Microarray construction and design

For the construction of AppChip2, 2033 ORFs from the complete genome sequence of *A. pleuropneumoniae* serotype 5b strain L20, representing more than 95% of all ORFs with a length greater than 160 nt, were amplified and spotted in duplicate on the chip. Spotted sheared genomic DNA from *A. pleuropneumoniae* L20 and porcine DNA are used as controls (GEO: GPL6658). Additional information concerning chip production is described by Gouré et al. [13].

2.4.3. Microarray hybridizations

cDNA synthesis and microarray hybridizations were performed as described [6]. Briefly, equal amounts (15 µg) of test RNA and control RNA were used to set up a standard reverse transcription reaction using random octamers (BioCorp, Montreal, QC, Canada), SuperScript II (Invitrogen, Carlsbad, CA, USA) and aminoallyl-dUTP (Sigma, St. Louis, MO, USA), and the resulting cDNA was indirectly labelled using a monofunctional NHS-ester Cy3 or Cy5 dye (Amersham, Buckinghamshire, UK). The labelling efficiency was assessed spectrophotometrically. Labelled samples were then combined and added to the AppChip2 for overnight hybridization. Five hybridizations were performed for the serotype 1 strain S4074 BHI-A versus BHI-B experiments. All slides were scanned using a Perkin-Elmer ScanArray Express scanner.

2.4.4. Microarray analysis and bioinformatics

Microarray data analysis was conducted with the TM4 Suite of software from the J. Craig Venture Institute [30] as described by Deslandes et al. [9]. Briefly, raw data was first generated using SpotFinder v.3.1.1. Locally weighted linear regression (lowess) was then performed in the Microarray Data Analysis System (MIDAS) in order to normalize the data. The Significance Analysis of Microarray (SAM) algorithm [33], which is implemented in TIGR Microarray Expression Viewer (TMEV), was used to generate a list of differentially expressed genes. During SAM analysis, a false discovery rate (FDR) of 0% was estimated for the serotype 1 strain S4074 BHI-A versus BHI-B experiments.

2.5. Effects of DspB and zinc on biofilm formation

Biofilms were grown for 6 or 24 h in BHI-B as described above. The wells were washed with water and then filled with 100 µL of PBS containing 0.2, 2.0 or 20 µg/mL of DspB (Kane Biotech Inc, Winnipeg, MB, Canada) as described by Izano et al. [17]. After incubation at 37 °C for 5 min, the wells were rinsed with water and stained with crystal violet. To monitor the effect of zinc on biofilm formation, bacteria were grown for 6 or 24 h in BHI-B supplemented with 50–250 µg/mL of $ZnCl_2$.

2.6. Statistical analysis

The statistical significance (p value) of differences in biofilm phenotypes (mean optical density values) was determined by a paired, one-tailed t-test using GraphPad Prism version 4.0 (GraphPad Software, San Diego, CA, USA).

3. RESULTS

3.1. Biofilm formation and growth conditions

The ability of the *A. pleuropneumoniae* serotype 1 reference strain S4074 to form biofilms was evaluated using different growth media (Fig. 1). No biofilm was present in the wells containing bacterial cells grown in LB broth while only a slight biofilm was observed in wells containing cells grown in TSB, MH or BHI-A broths after 24 h of incubation. However a pronounced biofilm ($p < 0.01$) was formed when strain S4074 was grown in BHI-B broth. This was not due to an increased growth in BHI-B compared to BHI-A as similar growth curves were observed in both media.

We then evaluated biofilm formation by all the reference strains of *A. pleuropneumoniae* after growth for 6 or 24 h in BHI-B. Similarly to what was observed with the serotype 1, we found that growth in BHI-B, but not BHI-A, allows biofilm formation in reference strains representing serotypes 4, 5a and 14. In addition

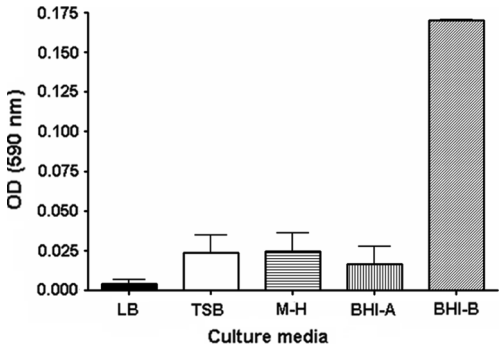

Figure 1. Biofilm formation by *A. pleuropneumoniae* serotype 1 reference strain S4074 grown in different culture media using the crystal violet staining protocol described in Materials and methods. LB: Luria-Bertani; TSB: tryptic soy broth; M-H: Mueller Hinton; BHI: brain heart infusion.

to the already reported biofilm formation in serotypes 5b and 11, we also observed biofilms for serotype 3 and 12 reference strains. Moreover, biofilm formation (OD_{590nm} > 0.1) was observed in 20 (54%) of the 37 fresh field isolates of serotypes 1, 5, 7 and 15 that were tested (Fig. 2). In general, serotypes 5a, 5b and 7 field isolates tend to form more biofilms (mean OD of 1.15, 1.47 and 1.47 after 24 h) than isolates from serotypes 1 and 15 (mean OD of 0.36 and 0.80 after 24 h).

When *A. pleuropneumoniae* strain S4074 grown in BHI-A (no or slight biofilm) was transferred to BHI-B we observed the formation of a pronounced biofilm ($p < 0.05$). When these cells were then transferred back to BHI-A, the phenotype returned to a slight biofilm ($p < 0.05$). This was also observed with field isolates representing different serotypes (data not shown).

3.2. Scanning laser confocal microscopy

We observed that for many reference strains, including strain S4074, and field isolates, pronounced biofilms were present after a short incubation period of only 6 h (Fig. 2). The biofilm was visualized by confocal laser scanning microscopy using a fluorescent probe (WGA-Oregon Green) specific to the PGA matrix polysaccharide (Fig. 3). It is evident from these micrographs that *A. pleuropneumoniae* strain S4074 does not form biofilm when grown in BHI-A while a thick PGA matrix is formed by *A. pleuropneumoniae* serotype 5b strain L20 grown in the same condition. However, both strains showed a pronounced biofilm when grown in BHI-B. In the case of strain S4074, the biofilm is even more important after 6 h than 24 h of incubation (Fig. 3). Because scanning laser confocal microscopy allows optical sectioning of the biofilm either in the horizontal or the vertical dimension it is possible to evaluate the thickness of the biofilm. We evaluated the thickness of *A. pleuropneumoniae* strain S4074 biofilm to be of ~ 25 µm after growth in BHI-B for 6 h (Fig. 3C) and even greater (~ 65 µm) for *A. pleuropneumoniae* strain L20.

3.3. Transcriptomic profiling under different growth conditions

To assess the transcriptional response of *A. pleuropneumoniae* S4074 after growth in BHI-B compared to BHI-A, transcript profiling experiments using DNA microarrays were performed. Overall, 232 genes were significantly differentially expressed during growth in BHI-B; 152 being up-regulated and 80 being down-regulated (Tab. II). The genes that showed the highest level of up-regulation after growth in BHI-B belonged to the "amino acid biosynthesis", "energy metabolism", "transport and binding proteins", "cell envelope" and "hypothetical/unknown/unclassified" functional classes (Fig. 4). Genes such as *tadC* and *tadD* (tight adherence proteins C and D), genes with homology to autotransporter adhesins (APL_0443 and APL_0104) as well as genes *pgaABC* involved in PGA biosynthesis were up-regulated after growth in BHI-B. A cluster of genes involved in dipeptide transport (*dppABCDF*) and genes involved in the synthesis of an urease (*ureAEFG*) were also up-regulated. Down-regulated genes after growth in BHI-B mostly belonged to the "transport and binding proteins", "cell envelope", "protein synthesis" and "hypothetical/

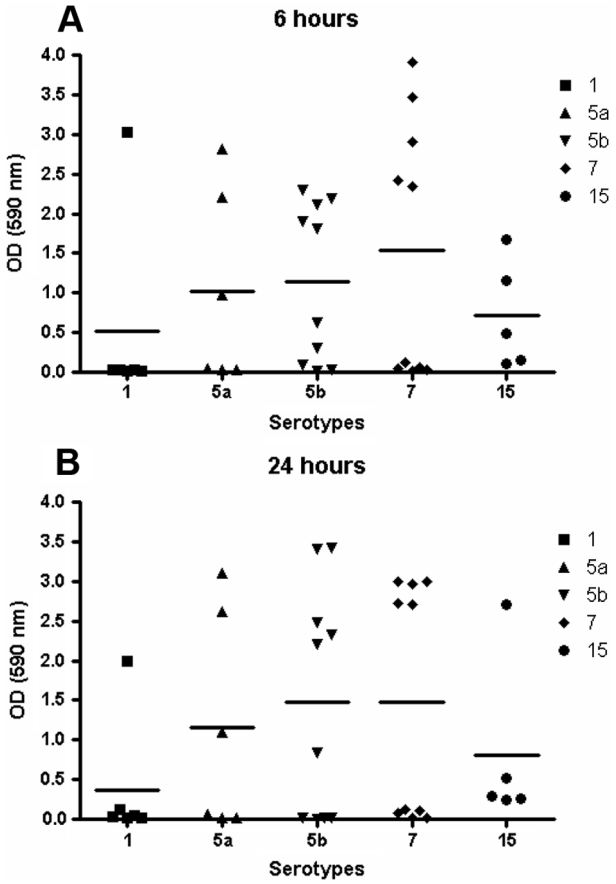

Figure 2. Thirty-seven independent fresh field isolates of *A. pleuropneumoniae* (representing serotypes 1, 5, 7 and 15) were tested for their ability to form biofilms when grown for 6 h (A) and 24 h (B) in BHI-B using the microtiter plate assay.

unknown/unclassified" functional classes. Most notably, *cys* genes involved in sulphate transport systems were down-regulated, as well as a gene (APL_1096) sharing 59% identity with the DspB gene of *A. actinomycetemcomitans*.

3.4. Effect of DspB on biofilm formation

Enzymatic treatment with DspB of biofilms of *A. pleuropneumoniae* strains S4074 and L20 grown for 6 or 24 h almost completely dispersed them ($p < 0.05$) confirming the presence of PGA in the biofilm matrix.

3.5. Effect of zinc on biofilm formation

Chemical analysis showed differences in some divalent cations concentration between BHI-A (Fe < 0.10 ppm, Zn 2.03 ppm) and BHI-B (Fe 0.10 ppm, Zn 1.75 ppm) while no differences were observed for others (Ca, Cu, Mg, Mn). We therefore hypothesized that the difference in biofilm formation observed after growth in BHI-B compared to BHI-A might be due to cations concentration. Since the concentration of zinc was found to be higher in BHI-A (no or slight biofilm) we tested a

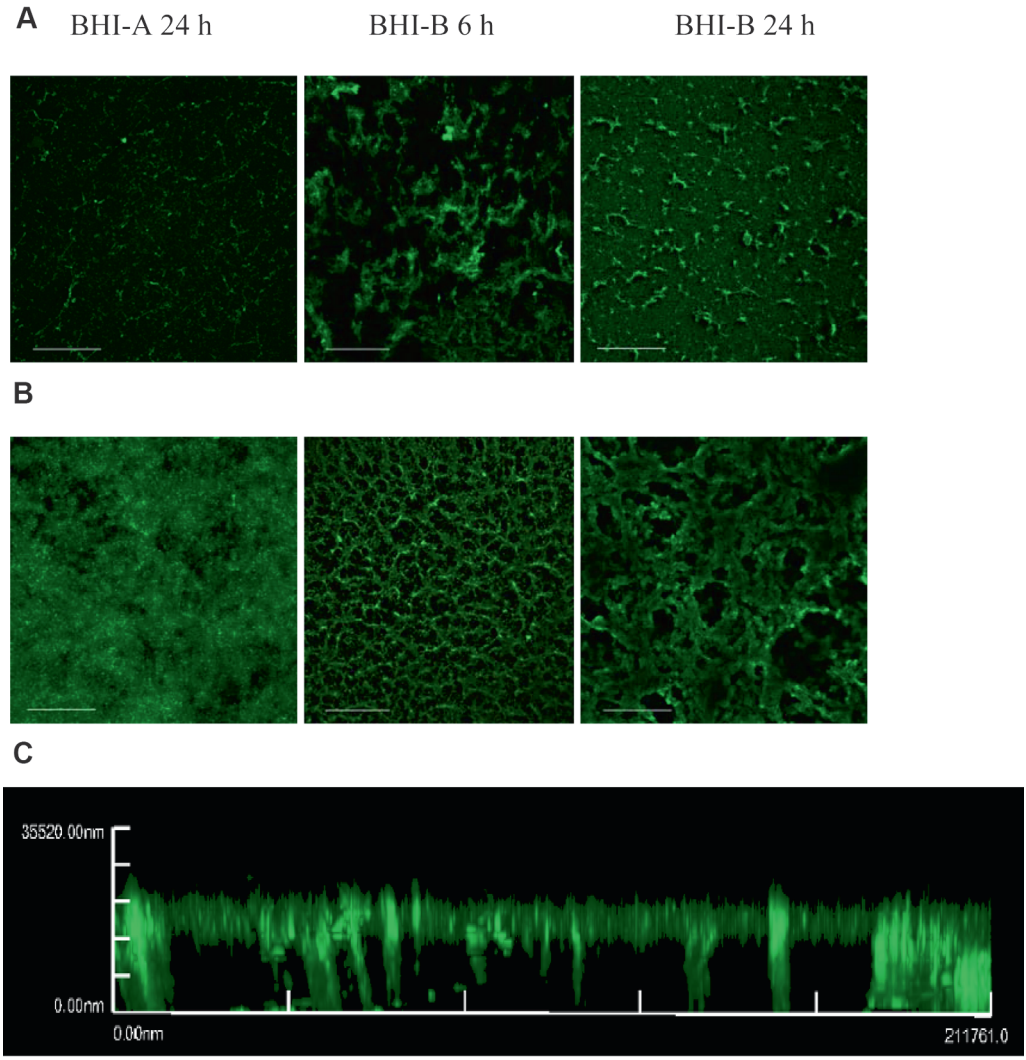

Figure 3. Confocal scanning laser microscopic images of *A. pleuropneumoniae* serotype 1 strain S4074 (A and C) and serotype 5b strain L20 (B) biofilms stained with WGA-Oregon Green 488. (C) Stack of sections through the X–Z plane of a biofilm formed after 6 h in BHI-B. Bars = 50 µm.

possible inhibitory effect of this cation on biofilm formation. The addition of $ZnCl_2$ to BHI-B inhibited, in a dose-dependent manner, the formation of biofilms by *A. pleuropneumoniae* strains S4074 and L20 (Fig. 5). A complete inhibition ($p < 0.01$) was observed when 100 µg/mL of $ZnCl_2$ was added to BHI-B, a concentration which did not affect growth after 24 h (data not shown). A similar inhibition was also observed with the addition of $ZnSO_4$, ZnO, and $Zn_3(PO_4)_2$ but not with $MgCl_2$ or $CaCl_2$ thus confirming that the inhibition was due to the addition of zinc. Biofilm formation in *A. actinomycetemcomitans* was also inhibited

Table II. *A. pleuropneumoniae* strain S4074 genes that are up- or down-regulated after growth in BHI-B compared to growth in BHI-A.

Locus tag	Gene	Description	Fold change
Amino acid biosynthesis			
APL_0728	*ilvH*	Acetolactate synthase small subunit	5.707
APL_0662	*aspC*	Putative aspartate aminotransferase	5.324
APL_0427	*gdhA*	NADP-specific glutamate dehydrogenase	4.943
APL_0727	*ilvI*	Acetolactate synthase large subunit	4.204
APL_0099	*ilvG*	Acetolactate synthase isozyme II large subunit (AHAS-II)	3.915
APL_1499	*thrC*	Threonine synthase	3.198
APL_0097	*ilvD*	Dihydroxy-acid dehydratase	3.142
APL_0393	*leuA*	2-isopropylmalate synthase	3.000
APL_0098	*ilvM*	Acetolactate synthase isozyme II small subunit (AHAS-II)	2.934
APL_2027	*hisF*	Imidazole glycerol phosphate synthase subunit hisF	2.833
APL_0702	*serC*	Phosphoserine aminotransferase	2.788
APL_0432	*leuB*	3-isopropylmalate dehydrogenase	2.643
APL_0899	*dapA*	Dihydrodipicolinate synthase	2.401
APL_0211	*glyA*	Glycine/serine hydroxymethyltransferase	2.398
APL_0133	*cysB*	HTH-type transcriptional regulator CysB	2.340
APL_1853	*ilvC*	Ketol-acid reductoisomerase	2.313
APL_0072	*ilvE*	Branched-chain-amino-acid aminotransferase	2.001
APL_0859	*trpCF*	Tryptophan biosynthesis protein trpCF	1.883
APL_2025	*hisH*	Imidazole glycerol phosphate synthase subunit hisH	1.777
APL_2026	*hisA*	Phosphoribosylformimino-5-aminoimidazole carboxamide ribotide isomerase	1.739
APL_1198	*APL_1198*	Putative NAD(P)H nitroreductase	1.708
APL_0139	*leuC*	3-isopropylmalate dehydratase large subunit 2	1.605
APL_1230	*serB*	Phosphoserine phosphatase	1.438
APL_0620	*aroG*	Phospho-2-dehydro-3-deoxyheptonate aldolase	1.428
APL_1873	*dapE*	Succinyl-diaminopimelate desuccinylase	1.380
Biosynthesis of cofactors, prosthetic groups, and carriers			
APL_0207	*Dxs*	1-deoxy-D-xylulose-5-phosphate synthase (DXPS)	−1.555
APL_1461	*menA*	1,4-dihydroxy-2-naphthoateoctaprenyltransferase	−1.631
APL_0382	*ribD*	Riboflavin biosynthesis protein	−1.726
APL_1408	*gshA*	Glutathione biosynthesis bifunctional protein GshAB	−1.789
Cell envelope			
APL_1494	*ftpA*	Fine tangled pili major subunit	5.705
APL_1921	*pgaA*	Biofilm PGA synthesis protein PgaA precursor	5.308
APL_0460	*plpD*	Lipoprotein Plp4	3.801
APL_1923	*pgaC*	Biofilm PGA synthesis N-glycosyltransferase PgaC	3.591
APL_1922	*pgaB*	Biofilm PGA synthesis lipoprotein PgaB precursor	3.093
APL_0006	*ompP2A*	Outer membrane protein P2	2.515
APL_0550	*tadC*	Tight adherence protein C	1.985
APL_0442	*sanA*	SanA protein	1.776
APL_0549	*tadD*	Tight adherence protein D	1.749
APL_0332	*hlpB*	Lipoprotein HlpB	1.627
APL_1364	*gmhA*	Putative phosphoheptose isomerase	1.386
APL_0873	*rlpB*	Putative rare lipoprotein B	−1.391

Continued on next page

Table II. Continued.

Locus tag	Gene	Description	Fold change
APL_1028	*APL_1028*	Possible lipooligosaccharide N-acetylglucosamine glycosyltransferase	−1.445
APL_0747	*mepA*	Penicillin-insensitive murein endopeptidase precursor	−1.446
APL_0436	*mreC*	Rod shape-determining protein MreC	−1.585
APL_1086	*ompW*	Outer membrane protein W precursor	−1.606
APL_1029	*APL_1029*	Hypothetical protein	−1.650
APL_1424	*oxaA*	Inner membrane protein OxaA	−1.772
APL_0933	*ompP1*	Putative outer membrane protein precursor	−2.808
Cellular processes			
APL_1489	*Tpx*	Putative thiol peroxidase	2.252
APL_0988	*hktE*	Catalase	−1.461
APL_0669	*APL_0669*	Putative iron dependent peroxidase	−1.483
APL_1442	*apxID*	RTX-I toxin secretion component	−1.506
APL_1346	*ftsY*	Cell division protein FtsY-like protein	−1.530
Central intermediary metabolism			
APL_1615	*Gst*	Putative glutathione S-transferase	3.269
APL_1614	*ureE*	Urease accessory protein UreE	2.601
APL_1613	*ureF*	Urease accessory protein UreF	2.478
APL_1612	*ureG*	Urease accessory protein UreG	2.165
APL_1618	*ureA*	Urease gamma subunit UreA	1.653
DNA metabolism			
APL_1931	*tagI*	3-methyladenine-DNA glycosidase	−1.500
APL_1474	*dnaG*	DNA primase	−1.551
APL_1282	*dnaQ*	DNA polymerase III subunit	−1.579
APL_1255	*parE*	DNA topoisomerase IV subunit	−1.630
APL_1505	*holC*	DNA polymerase III subunit	−1.663
Energy metabolism			
APL_1197	*APL_1197*	3-hydroxyacid dehydrogenase	3.100
APL_0841	*pntB*	NAD(P) transhydrogenase subunit beta	2.726
APL_1908	*xylA*	Xylose isomerase	2.243
APL_0894	*fdxH*	Formate dehydrogenase, iron-sulfur subunit	2.161
APL_1425	*napC*	Cytochrome c-type protein NapC	2.159
APL_1799	*torC*	Pentahemic c-type cytochrome	2.156
APL_0892	*fdxG*	Formate dehydrogenase, nitrate-inducible, major subunit	2.116
APL_1798	*torA*	Trimethylamine-N-oxide reductase precursor	1.977
APL_0381	*glpC*	Anaerobic glycerol-3-phosphate dehydrogenase subunit C	1.919
APL_0842	*pntA*	NAD(P) transhydrogenase subunit alpha	1.903
APL_0895	*fdnI*	Formate dehydrogenase, cytochrome b556 subunit	1.816
APL_1208	*adhC*	Putative alcohol dehydrogenase class 3	1.801
APL_0971	*APL_0971*	Putative acyl CoA thioester hydrolase	1.796
APL_0652	*manB*	Phosphomannomutase	1.677
APL_0483	*APL_0483*	Predicted nitroreductase	1.668
APL_0142	*glxK*	Glycerate kinase	1.564
APL_0452	*sucC*	Succinyl-CoA synthetase beta chain	1.515
APL_0461	*APL_0461*	Predicted hydrolases of the HAD superfamily	1.456

Continued on next page

Table II. Continued.

Locus tag	Gene	Description	Fold change
APL_0687	*Dld*	D-lactate dehydrogenase	1.439
APL_1510	*gpsA*	Glycerol-3-phosphate dehydrogenase (NAD(P)+)	1.414
APL_1427	*napH*	Ferredoxin-type protein NapH-like protein	1.360
APL_0789	*APL_0789*	Dioxygenase	1.253
APL_0983	*tktA*	Transketolase 2	1.233
APL_1036	*pflB*	Formate acetyltransferase	−1.653
APL_1498	*mgsA*	Methylglyoxal synthase	−1.790
APL_1840	*ubiC*	4-hydroxybenzoate synthetase (chorismate lyase)	−1.952
APL_0857	*sdaA*	L-serine dehydratase	−3.016
Fatty acid and phospholipid metabolism			
APL_1407	*Psd*	Phosphatidylserine decarboxylase	−1.419
APL_1384	*fabH*	3-oxoacyl-[acyl-carrier-protein] synthase 3	−1.826
APL_1385	*plsX*	Fatty acid/phospholipid synthesis protein PlsX	−2.706
Mobile and extrachromosomal element functions			
APL_1056	*APL_1056*	Transposase	1.560
APL_0985	*APL_0985*	Transposase	1.271
Protein fate			
APL_0871	*pepE*	Peptidase E	2.551
APL_1101	*pepA*	Putative cytosol aminopeptidase	1.913
APL_0254	*pepD*	Aminoacyl-histidine dipeptidase	1.903
APL_1883	*ptrA*	Protease 3 precursor	1.680
APL_0928	*hscB*	Co-chaperone protein HscB-like protein	1.377
APL_1068	*secF*	Protein-export membrane protein SecF	−1.496
APL_0321	*dsbB*	Disulfide bond formation protein B	−1.557
APL_1035	*pflA*	Pyruvate formate-lyase 1-activating enzyme	−1.774
Protein synthesis			
APL_1821	*rpmE*	50S ribosomal protein L31	2.211
APL_0484	*rimK*	Ribosomal protein S6 modification protein	1.533
APL_1781	*rpsM*	30S ribosomal protein S13	−1.401
APL_0205	*APL_0205*	Predicted rRNA methyltransferase	−1.538
APL_0399	*ksgA*	Dimethyladenosine transferase	−1.578
APL_0679	*glnS*	Glutaminyl-tRNA synthetase	−1.584
APL_0641	*truB*	tRNA pseudouridine synthase B	−1.742
APL_1383	*trmB*	tRNA (guanine-N(7)-)-methyltransferase	−1.756
APL_0574	*APL_0574*	tRNA-specific adenosine deaminase	−1.778
APL_0723	*Tgt*	Queuine tRNA-ribosyltransferase	−1.937
Purines, pyrimidines, nucleosides, and nucleotides			
APL_0958	*purH*	Bifunctional purine biosynthesis protein PurH	1.856
APL_0593	*guaB*	Inosine-5′-monophosphate dehydrogenase	1.485
APL_1343	*Cdd*	Cytidine deaminase	1.278
APL_1014	*deoD*	Purine nucleoside phosphorylase DeoD-like protein	−1.430
APL_0351	*Ndk*	Nucleoside diphosphate kinase	−1.531
APL_1839	*Udp*	Uridine phosphorylase	−1.617
APL_1075	*purA*	Adenylosuccinate synthetase	−1.762

Continued on next page

Table II. Continued.

Locus tag	Gene	Description	Fold change
Regulatory functions			
APL_0059	*narP*	Nitrate/nitrite response regulator protein	2.552
APL_0823	*glpR*	Glycerol-3-phosphate regulon repressor	1.908
APL_1295	*argR*	Arginine repressor	1.896
APL_0126	*APL_0126*	HIT-like protein	1.580
APL_0395	*rseA*	Putative sigma-E factor negative regulatory protein	1.524
APL_1668	*rbsR*	Ribose operon repressor	1.302
APL_1270	*sprT*	Putative SprT-like protein	−1.483
APL_1233	*malT*	HTH-type transcriptional regulator MalT	−1.484
APL_1540	*tldD*	TldD-like protein	−1.578
Transcription			
APL_0560	*rhlB*	ATP-dependent RNA helicase RhlB	1.409
APL_0423	*rnhA*	Ribonuclease HI	1.345
APL_0201	*nusB*	Transcription antitermination protein NusB	−1.457
Transport and binding proteins			
APL_0967	*gltS*	Sodium/glutamate symport carrier protein	4.155
APL_0377	*glpT*	Glycerol-3-phosphate transporter	3.247
APL_0064	*dppA*	Periplasmic dipeptide transport protein	3.168
APL_0869	*abgB*	Aminobenzoyl-glutamate utilization-like protein	3.004
APL_1857	*merP*	Copper chaperone MerP	2.911
APL_0068	*dppF*	Dipeptide transport ATP-binding protein DppF	2.860
APL_1665	*gntP_1*	Gluconate permease	2.723
APL_0066	*dppC*	Dipeptide transport system permease protein DppC	2.640
APL_1440	*znuA*	High-affinity zinc uptake system protein ZnuA precursor	2.600
APL_0065	*dppB*	Dipeptide transport system permease protein DppB	2.229
APL_0067	*dppD*	Dipeptide transport ATP-binding protein DppD	2.036
APL_1448	*afuC*	Ferric ABC transporter ATP-binding protein	1.855
APL_1319	*ptsB*	PTS system sucrose-specific EIIBC component	1.744
APL_1320	*thiQ*	Thiamine transport ATP-binding protein ThiQ	1.569
APL_1622	*cbiM*	Predicted ABC transport permease protein CbiM	1.433
APL_1620	*cbiO*	Predicted ABC transport ATP-binding protein CbiO	1.417
APL_1173	*pnuC*	Nicotinamide mononucleotide transporter	1.408
APL_0749	*APL_0749*	Potassium efflux system KefA	−1.436
APL_1212	*tehA*	Tellurite resistance protein TehA	−1.543
APL_0716	*APL_0716*	Iron(III) ABC transporter, permease protein	−1.547
APL_1253	*APL_1253*	Putative sodium/sulphate transporter	−1.598
APL_1846	*cysT*	Sulfate transport system permease protein cysT	−1.684
APL_0191	*APL_0191*	Predicted Na+-dependent transporter of the SNF family	−1.751
APL_1083	*arcD*	Putative arginine/ornithine antiporter	−1.786
APL_2016	*fhuA*	Ferrichrome-iron receptor FhuA	−2.031
APL_1847	*cysW*	Sulfate transport system permease protein cysW	−2.195
APL_1844	*cysN*	Sulphate adenylate transferase subunit 1	−2.375
APL_1848	*cysA*	Sulfate/thiosulfate import ATP-binding protein cysA	−2.401
APL_1843	*cysJ*	Sulfite reductase [NADPH] flavoprotein alpha-component	−2.757
APL_1127	*APL_1127*	Predicted Na+/alanine symporter	−3.402

Continued on next page

Table II. Continued.

Locus tag	Gene	Description	Fold change
Hypothetical/unknown/unclassified			
APL_1100	*APL_1100*	Hypothetical protein	3.395
APL_0920	*APL_0920*	Hypothetical protein	2.835
APL_1882	*APL_1882*	Hypothetical protein	2.776
APL_1856	*APL_1856*	Hypothetical protein	2.775
APL_1855	*APL_1855*	Hypothetical protein	2.763
APL_0443	*APL_0443*	Autotransporter adhesin	2.762
APL_1252	*APL_1252*	Hypothetical protein	2.739
APL_0134	*APL_0134*	Hypothetical protein	2.681
APL_0836	*APL_0836*	Putative transcriptional regulator	2.661
APL_1588	*APL_1588*	Predicted TRAP transporter solute receptor	2.464
APL_1491	*APL_1491*	Hypothetical protein	2.282
APL_0104	*APL_0104*	Autotransporter adhesin	2.231
APL_1069	*ftnA*	Ferritin-like protein 1	2.194
APL_1059	*APL_1059*	Hypothetical transposase-like protein	2.172
APL_1690	*APL_1690*	Inner membrane protein	2.168
APL_0245	*APL_0245*	Transferrin binding protein-like solute binding protein	2.097
APL_1191	*namA*	NADPH dehydrogenase	2.078
APL_1948	*APL_1948*	Hypothetical protein	2.061
APL_0870	*APL_0870*	Putative C4-dicarboxylate transporter	2.034
APL_0643	*APL_0643*	Hypothetical protein	2.029
APL_1743	*APL_1743*	Ser/Thr protein phosphatase family protein	1.999
APL_0426	*APL_0426*	Hypothetical protein	1.994
APL_1791	*APL_1791*	Putative periplasmic iron/siderophore binding protein	1.944
APL_0970	*APL_0970*	Hypothetical protein	1.908
APL_1070	*ftnB*	Ferritin-like protein 2	1.907
APL_1894	*APL_1894*	Hypothetical protein	1.907
APL_1374	*APL_1374*	Hypothetical protein	1.803
APL_1206	*APL_1206*	Plasmid stability-like protein	1.794
APL_1881	*APL_1881*	Hypothetical protein	1.792
APL_0038	*APL_0038*	Hypothetical protein	1.730
APL_1355	*APL_1355*	Hypothetical protein	1.716
APL_0471	*APL_0471*	Hypothetical protein	1.707
APL_1438	*APL_1438*	Hypothetical protein	1.689
APL_1437	*APL_1437*	Hypothetical protein	1.643
APL_1423	*APL_1423*	Hypothetical protein	1.612
APL_0125	*APL_0125*	Hypothetical protein	1.608
APL_0096	*APL_0096*	Zinc transporter family protein ZIP	1.592
APL_0220	*APL_0220*	Putative lipoprotein	1.583
APL_1934	*APL_1934*	Hypothetical protein	1.570
APL_1574	*APL_1574*	Hypothetical protein	1.543
APL_0036	*APL_0036*	Hypothetical protein	1.533
APL_0222	*APL_0222*	Putative lipoprotein	1.518
APL_1088	*APL_1088*	Hypothetical protein	1.512
APL_1207	*APL_1207*	Hypothetical protein	1.510
APL_0463	*APL_0463*	Predicted sortase and related acyltransferases	1.448
APL_1859	*APL_1859*	Probable NADH-dependent butanol dehydrogenase 1	1.448
APL_1828	*APL_1828*	PilT protein-like protein	1.447

Continued on next page

Table II. Continued.

Locus tag	Gene	Description	Fold change
APL_0433	*msrB*	Methionine sulfoxide reductase B	1.415
APL_1189	*APL_1189*	Hypothetical protein	1.393
APL_0090	*APL_0090*	Hypothetical protein	1.360
APL_1709	*APL_1709*	Hypothetical protein	−1.307
APL_0357	*APL_0357*	Hypothetical protein	−1.328
APL_1380	*APL_1380*	Hypothetical protein	−1.394
APL_1729	*APL_1729*	Hypothetical protein	−1.401
APL_1062	*APL_1062*	Hypothetical protein	−1.468
APL_0179	*APL_0179*	Hypothetical protein	−1.481
APL_0940	*APL_0940*	Hypothetical protein	−1.482
APL_1273	*APL_1273*	Putative fimbrial biogenesis and twitching motility protein PilF-like protein	−1.488
APL_1131	*APL_1131*	Hypothetical protein	−1.540
APL_0583	*APL_0583*	Hypothetical protein	−1.585
APL_1096	*APL_1096*	Hypothetical protein (59% ID dispersine B)	−1.594
APL_0936	*APL_0936*	Hypothetical protein	−1.616
APL_1115	*APL_1115*	Hypothetical protein	−1.639
APL_0811	*APL_0811*	Hypothetical protein	−1.682
APL_1898	*ap2029*	Hypothetical protein	−1.798
APL_1654	*gidB*	Methyltransferase GidB	−1.816
APL_0340	*APL_0340*	Hypothetical protein	−1.893
APL_1381	*APL_1381*	Hypothetical protein	−1.926
APL_0053	*typA*	GTP-binding protein	−2.043
APL_1681	*APL_1681*	Hypothetical protein	−2.233

by zinc (data not shown). Interestingly, genes potentially involved in zinc transport (*znuA* and APL_0096) were up-regulated after growth in BHI-B (Tab. II).

4. DISCUSSION

Biofilm formation is an important virulence trait of many bacterial pathogens including *A. pleuropneumoniae*. It has been previously reported that only 2 of the 15 *A. pleuropneumoniae* reference strains, representing serotypes 5b and 11, were able to form a biofilm in vitro [21]. We observed however an increased stickiness of colonies when strain *A. pleuropneumoniae* S4074 was grown on plates made of BHI from one of two different suppliers. In addition, Li et al. [24] recently observed slight biomass of biofilm when the *A. pleuropneumoniae* serotype 1 reference strain S4074 was grown in serum-free TSB and that an enhanced biofilm formation was observed in *luxS* [24] and *hns* [8] mutants of *A. pleuropneumoniae* S4074. These observations brought us to re-evaluate biofilm formation by strain *A. pleuropneumoniae* S4074 under different growth conditions using a standard microtiter plate and crystal violet staining protocol. Our data indicate that strain S4074 has the ability to form a pronounced biofilm when grown in the appropriate conditions, and that the biofilm was sensitive to DspB treatment and can be inhibited by zinc. Transition from a biofilm-positive to a biofilm-negative phenotype is not irreversible in contrast to what was reported by Kaplan and Mulks [21] under different conditions.

Transcript profiling experiments using DNA microarrays indicated that overall, 232 genes were significantly differentially expressed during growth in BHI-B. Genes such as *tadC*, *tadD*, genes with homology to autotransporter adhesins as well as genes *pgaABC* involved in PGA biosynthesis were up-regulated after

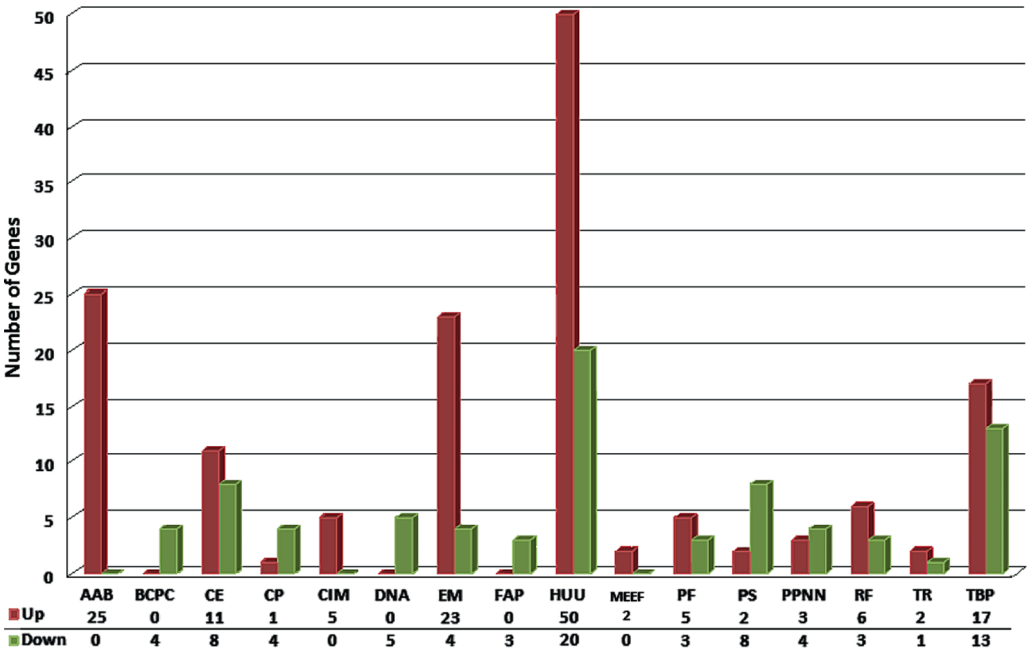

Figure 4. Functional classification of the differentially expressed genes during growth of *A. pleuropneumoniae* S4074 in BHI-B according to TIGRFAM. AAB: amino acids biosynthesis; BCPC: biosynthesis of cofactors, prosthetic groups and carriers; CE: cell envelope; CP: cellular processes; CIM: central intermediary metabolism; DNA: DNA metabolism; EM: energy metabolism; FAPM: fatty acid and phospholipid metabolism; HUU: hypothetical proteins/unclassified/unknown; MEEF: mobile and extrachromosomal element functions; PF: protein fate; PS: protein synthesis; PPNN: purines, pyrimidines, nucleosides and nucleotides; RF: regulatory functions; TR: transcription and TBP: transport and binding proteins.

growth in BHI-B. While we can hypothesize that these genes might be important for the formation of the biofilm itself, it is also interesting to note that many of the same genes (*tadB*, *rcpA*, gene APL_0443 with high homology to the Hsf autotransporter adhesin of *Haemophilus influenzae* as well as genes *pgaBC* involved in biofilm biosynthesis) were up-regulated, when the transcriptomic profile of *A. pleuropneumoniae* was determined after contact with porcine lung epithelial cells [1], thus emphasizing the possible importance of biofilm formation for the establishment of the infection.

Initial steps in biofilm development require the transcription, early on, of genes involved in reversible attachment and motility, before a subsequent switch towards the transcription of genes involved in the irreversible attachment of bacteria [35]. This second irreversible attachment might require the synthesis of adhesive organelles, such as the curli fibers (*csg* genes). Interestingly, gene APL_0220 is a putative lipoprotein of the CsgG family, responsible for the transport and assembly of curli fibers. The up-regulation of other genes possibly involved in adhesion processes (*tadC*, *tadD*, Hsf homolog APL_0443) might indicate that bacterial cells were entering or in the middle of this irreversible attachment phase. In *A. actinomycetemcomitans*, the Tad locus is essential for biofilm formation [32]. The fact that the transcription of a zinc-specific transporter (*znuA*) was increased, combined with the decrease in transcription of an hypothetical Zn-dependant

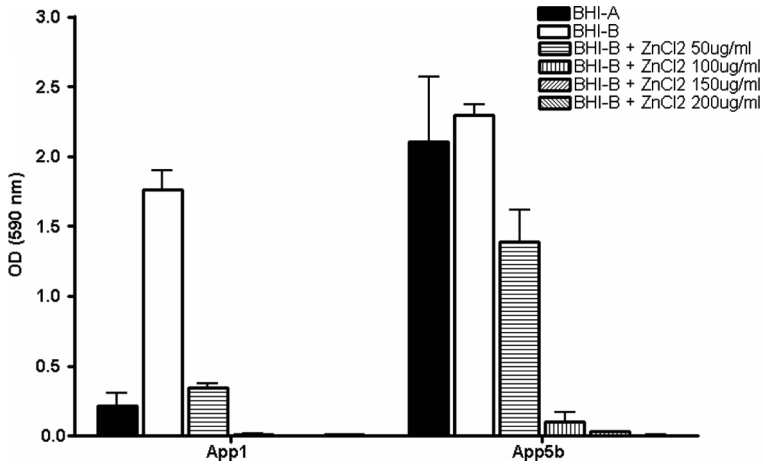

Figure 5. Effect of the addition of $ZnCl_2$ on biofilm formation by *A. pleuropneumoniae* serotype 1 strain S4074 (App1) and serotype 5b strain L20 (App5b) grown for 6 h.

protease (APL_1898) and lower concentration of this metal in BHI-B lead us to believe that Zn restriction might be a signal leading to increase biofilm formation.

It is tempting to speculate that growth in BHI-B affected the expression of regulators which in turn affected PGA expression and biofilm formation. Indeed, it has been recently shown that an enhanced biofilm formation was observed in a *hns* mutant of *A. pleuropneumoniae* strain S4074 [8] and that over-expression of RpoE in a *rseA* mutant is sufficient to alleviate repression of biofilm formation by H-NS[1]. However, other genes have been shown to affect biofilm formation in *A. pleuropneumoniae*. An enhanced biofilm formation was observed in a quorum sensing (*luxS*) mutant [24] while a mutant in the ArcAB two-component system facilitating metabolic adaptation to anaerobicity (*arcA*) [5] and an autotransporter serine protease (AasP) mutant were deficient in biofilm formation [31]. It is interesting to note that many genes involved in branched-chain amino acid biosynthesis (*ilv* genes) were up-regulated after growth in BHI-B. Limitation of branched-chain amino acids was shown to be a cue for expression of a subset of in vivo induced genes in *A. pleuropneumoniae*, including not only genes involved in the biosynthesis of branched-chain amino acids, but also other genes that are induced during infection of the natural host [34].

Our data indicate that many strains of *A. pleuropneumoniae* have the ability to form biofilms under appropriate growth conditions. This is an important observation considering that *A. pleuropneumoniae* biofilm cells exhibit increased resistance to antibiotics compared to planktonic cells [17] and may also exhibit increased resistance to biocides [12]. Biofilms are often associated with chronic infections but the fact that *A. pleuropneumoniae* can form an important biofilm after only 6 h of incubation suggests that biofilm formation might also play a role in acute infections.

We have undertaken the screen of a large library of mini-*Tn10* isogenic mutants of *A. pleuropneumoniae* S4074 in order to identify other genes that are involved in biofilm

[1] Bosse J.T., Sinha S., O'Dwyer C.A., Rycroft A.N., Kroll J.S., Langford P.R., H-NS is a specific regulator of biofilm formation in *Actinobacillus pleuropneumoniae*, Proceedings of the International *Pasteurellaceae* Society meeting, Sorrento, Italy, 2008, p. 110.

formation and/or regulation. A better understanding of biofilm formation in *A. pleuropneumoniae* might lead to the development of molecules or strategies to interfere with biofilm formation and prevent infection in pigs. In that respect, we made an important, and unexpected, observation that zinc could completely inhibit biofilm formation in *A. pleuropneumoniae* and *A. actinomycetemcomitans*, which also synthesizes PGA [20]. We do not know at this time how zinc interferes with PGA biosynthesis and biofilm formation but some glycosyltransferases have been shown to be inhibited by zinc [23]. Hypozincemia which occurs during infection and inflammation [26] might therefore favour biofilm formation by *A. pleuropneumoniae*. Knowing that PGA functions as a biofilm matrix polysaccharide in phylogenetically diverse bacterial species such as *Staphylococcus aureus*, *S. epidermidis*, and *Escherichia coli* [20], it would be worth investigating whether zinc can also interfere with PGA biosynthesis in these other bacterial pathogens.

Acknowledgements. This work was supported by a discovery grant from the Natural Sciences and Engineering Research Council of Canada (DGPIN0003428) to M. Jacques. The authors would also like to acknowledge the contribution of Patrick Vincent for confocal microscopy.

REFERENCES

[1] Auger E., Deslandes V., Ramjeet M., Contreras I., Nash J.H., Harel J., et al., Host pathogen interactions of *Actinobacillus pleuropneumoniae* with porcine lung and tracheal epithelial cells, Infect. Immun. (2009) 77:1426–1441.

[2] Bernstein J.A., Khodursky A.B., Lin P.H., Lin-Chao S., Cohen S.N., Global analysis of mRNA decay and abundance in *Escherichia coli* at single-gene resolution using two-color fluorescent DNA microarrays, Proc. Natl. Acad. Sci. USA (2002) 99:9697–9702.

[3] Blackall P.J., Klaasen H.L., van den Bosch H., Kuhnert P., Frey J., Proposal of a new serovar of *Actinobacillus pleuropneumoniae*: serovar 15, Vet. Microbiol. (2002) 84:47–52.

[4] Bosse J.T., Janson H., Sheehan B.J., Beddek A.J., Rycroft A.N., Kroll J.S., Langford P.R., *Actinobacillus pleuropneumoniae*: pathobiology and pathogenesis of infection, Microbes Infect. (2002) 4:225–235.

[5] Buettner F.F., Maas A., Gerlach G.-F., An *Actinobacillus pleuropneumoniae arcA* deletion mutant is attenuated and deficient in biofilm formation, Vet. Microbiol. (2008) 127:106–115.

[6] Carrillo C.D., Taboada E., Nash J.H., Lanthier P., Kelly J., Lau P.C., et al., Genome-wide expression analyses of *Campylobacter jejuni* NCTC11168 reveals coordinate regulation of motility and virulence by *flhA*, J. Biol. Chem. (2004) 279:20327–20338.

[7] Costerton J.W., Springer series on biofilms: the biofilm primer, Springer-Verlag, Berlin Heidelberg, 2007.

[8] Dalai B., Zhou R., Wan Y., Kang M., Li L., Li T., et al., Histone-like protein H-NS regulates biofilm formation and virulence of *Actinobacillus pleuropneumoniae*, Microb. Pathog. (2009) 46:128–134.

[9] Deslandes V., Nash J.H., Harel J., Coulton J.W., Jacques M., Transcriptional profiling of *Actinobacillus pleuropneumoniae* under iron-restricted conditions, BMC Genomics (2007) 8:72.

[10] Dubreuil J.D., Jacques M., Mittal K.R., Gottschalk M., *Actinobacillus pleuropneumoniae* surface polysaccharides: their role in diagnosis and immunogenicity, Anim. Health Res. Rev. (2000) 1:73–93.

[11] Frey J., RTX toxin-determined virulence in *Pasteurellaceae*, in: Kuhnert P., Christensen H. (Eds.), *Pasteurellaceae* – biology, genomics and molecular aspects, Caister Academic Press, Norfolk, UK, 2008, pp. 133–144.

[12] Ganeshnarayan K., Shah S.M., Libera M.R., Santostefano A., Kaplan J.B., Poly-N-acetylglucosamine matrix polysaccharide impedes fluid convection and transport of the cationic surfactant cetylpyridinium chloride through bacterial biofilms, Appl. Environ. Microbiol. (2009) 75:1308–1314.

[13] Gouré J., Findlay W.A., Deslandes V., Bouevitch A., Foote S.J., MacInnes J.I., et al., Microarray-based comparative genomic profiling of reference strains and selected Canadian field isolates of *Actinobacillus pleuropneumoniae*, BMC Genomics (2009) 10:88.

[14] Haesebrouck F., Chiers K., Van Overbeke I., Ducatelle R., *Actinobacillus pleuropneumoniae* infections in pigs: the role of virulence factors in pathogenesis and protection, Vet. Microbiol. (1997) 58:239–249.

[15] Hall-Stoodley L., Costerton J.W., Stoodley P., Bacterial biofilms: from the natural environment to infectious diseases, Nat. Rev. Microbiol. (2004) 2: 95–108.

[16] Inzana T.J., Swords W.E., Sandal I., Siddaramappa S., Lipopolysaccharides, biofilms and quorum sensing in *Pasteurellaceae*, in: Kuhnert P., Christensen H. (Eds.), *Pasteurellaceae* – biology, genomics and molecular aspects, Caister Academic Press, Norfolk, UK, 2008, pp. 177–195.

[17] Izano E.A., Sadovskaya I., Vinogradov E., Mulks M.H., Velliyagounder K., Ragunath C., et al., Poly-N-acetylglucosamine mediates biofilm formation and antibiotic resistance in *Actinobacillus pleuropneumoniae*, Microb. Pathog. (2007) 43:1–9.

[18] Jacques M., Role of lipo-oligosaccharides and lipopolysaccharides in bacterial adherence, Trends Microbiol. (1996) 4:408–409.

[19] Jacques M., Surface polysaccharides and iron-uptake systems in *Actinobacillus pleuropneumoniae*, Can. J. Vet. Res. (2004) 68:81–85.

[20] Kaplan J.B., Velliyagounder K., Ragunath C., Rohde H., Mack D., Knobloch J.K., Ramasubbu N., Genes involved in the synthesis and degradation of matrix polysaccharide in *Actinobacillus actinomycetemcomitans* and *Actinobacillus pleuropneumoniae* biofilms, J. Bacteriol. (2004) 186:8213–8220.

[21] Kaplan J.B., Mulks M.H., Biofilm formation is prevalent among field isolates of *Actinobacillus pleuropneumoniae*, Vet. Microbiol. (2005) 108:89–94.

[22] Kerrigan J.E., Ragunath C., Kandra L., Gyémant G., Liptak A., Janossy L., et al., Modeling and biochemical analysis of the activity of antibiofilm agent Dispersin B, Acta Biol. Hung. (2008) 59: 439–451.

[23] Koo H., Sheng J., Nguyen P.T., Marquis R.E., Co-operative inhibition by fluoride and zinc of glucosyltransferase production and polysaccharide synthesis by mutans streptococci in suspension cultures and biofilms, FEMS Microbiol. Lett. (2006) 254:134–140.

[24] Li L., Zhou R., Li T., Kang M., Wan Y., Xu Z., Chen H., Enhanced biofilm formation and reduced virulence of *Actinobacillus pleuropneumoniae luxS* mutant, Microb. Pathog. (2008) 45:192–200.

[25] Liu J., Tan C., Li J., Chen H., Xu P., He Q., et al., Characterization of ISApl1, an insertion element from *Actinobacillus pleuropneumoniae* field isolate in China, Vet. Microbiol. (2008) 132:348–354.

[26] Liuzzi J.P., Lichten L.A., Rivera S., Blanchard R.K., Aydemir T.B., Knutson M.D., et al., Interleukin-6 regulateds the zinc transporter Zip 14 in liver and contributes to the hypozincemia of the acute-phase response, Proc. Natl. Acad. Sci. USA (2005) 102:6843–6848.

[27] Merritt J.H., Kadouri D.E., O'Toole G.A., Growing and analyzing static biofilms, Curr. Protoc. Microbiol. (2005) 1B.1.1–1B.1.17.

[28] Ramjeet M., Deslandes V., St Michael F., Cox A.D., Kobisch M., Gottschalk M., Jacques M., Truncation of the lipopolysaccharide outer core affects susceptibility to antimicrobial peptides and virulence of *Actinobacillus pleuropneumoniae* serotype 1, J. Biol. Chem. (2005) 280:39104–39114.

[29] Ramjeet M., Cox A.D., Hancock M.A., Mourez M., Labrie J., Gottschalk M., Jacques M., Mutation in the lipopolysaccharide outer core biosynthesis gene, *galU*, affects LPS interaction with the RTX toxins ApxI and ApxII and cytolytic activity of *Actinobacillus pleuropneumoniae* serotype 1, Mol. Microbiol. (2008) 70:221–235.

[30] Saeed A.I., Sharov V., White J., Li J., Liang W., Bhagabati N., et al., TM4: a free, open-source system for microarray data management and analysis, Biotechniques (2003) 34:374–378.

[31] Tegetmeyer H.E., Fricke K., Baltes N., An isogenic *Actinobacillus pleuropneumoniae* AasP mutant exhibits altered biofilm formation but retain virulence, Vet. Microbiol. (2009) 137:392–396.

[32] Tomich M., Planet P.J., Figurski D.H., The Tad locus: postcards from the widespread colonization island, Nat. Rev. Microbiol. (2007) 5:363–375.

[33] Tusher V.G., Tibshirani R., Chu G., Significance analysis of microarrays applied to the ionizing radiation response, Proc. Natl. Acad. Sci. USA (2001) 98:5116–5121.

[34] Wagner T.K., Mulks M.H., A subset of *Actinobacillus pleuropneumoniae* in vivo induced promoters respond to branched-chain amino acids limitation, FEMS Immunol. Med. Microbiol. (2006) 48:192–204.

[35] Wood T.K., Insights on *Escherichia coli* biofilm formation and inhibition from whole-transcriptome profiling, Environ. Microbiol. (2009) 1:1–15.